



## Synthesis, biological evaluation, 3D-QSAR studies of novel aryl-2H-pyrazole derivatives as telomerase inhibitors

Yin Luo<sup>a,†</sup>, Shuai Zhang<sup>a,†</sup>, Ke-Ming Qiu<sup>a</sup>, Zhi-Jun Liu<sup>a</sup>, Yu-Shun Yang<sup>a</sup>, Jie Fu<sup>c</sup>, Wei-Qing Zhong<sup>b,\*</sup>, Hai-Liang Zhu<sup>a,\*</sup>

<sup>a</sup>State Key Laboratory of Pharmaceutical Biotechnology, Nanjing University, Nanjing 210093, P.R. China

<sup>b</sup>School of Pharmacy, Second Military Medical University, Shanghai 200433, P.R. China

<sup>c</sup>State Key Laboratory of Pollution Control & Resource Reuse, Nanjing University, Nanjing 210046, P.R. China

### ARTICLE INFO

#### Article history:

Received 4 November 2012

Revised 6 December 2012

Accepted 7 December 2012

Available online 20 December 2012

#### Keywords:

Aryl-2H-pyrazole  
Telomerase inhibitor  
Antiproliferative  
3D-QSAR

### ABSTRACT

A series of novel aryl-2H-pyrazole derivatives bearing 1,4-benzodioxan or 1,3-benzodioxole moiety were designed as potential telomerase inhibitors to enhance the ability of aryl-2H-pyrazole derivatives to inhibit telomerase, a target of anticancer. The telomerase inhibition tests showed that compound **16A** displayed the most potent inhibitory activity with IC<sub>50</sub> value of 0.9 μM for telomerase. The antiproliferative tests showed that compound **16A** exhibited high activity against human gastric cancer cell SGC-7901 and human melanoma cell B16-F10 with IC<sub>50</sub> values of 18.07 and 5.34 μM, respectively. Docking simulation showed that compound **16A** could bind well with the telomerase active site and act as telomerase inhibitor. 3D-QSAR model was also built to provide more pharmacophore understanding that could be used to design new agents with more potent telomerase inhibitory activity.

© 2012 Elsevier Ltd. All rights reserved.

In the early stage of life, telomerase is active and maintains telomere length and the chromosomal integrity of frequently dividing cells. During adulthood, telomerase keeps dormant in most somatic cells.<sup>1</sup> However, telomerase gets reactivated first and then works tirelessly to keep the short length of telomeres during the dividing stage of cancer cells, which leads to the long life of cancer cells.<sup>2</sup> The essential role of telomerase makes it an important target for the development of therapies to treat cancer and other age-associated disorders.<sup>3</sup>

Several applications were reported about 2H-pyrazole derivatives in pharmaceutical fields. According to the research papers, it showed that 2H-pyrazole derivatives have strong bioactivity, such as anticancer activity.<sup>4–7</sup> In 2005, Manna et al. reported a series of replacing aryl group 2H-pyrazole, which could directly combine and inhibit p-glycoprotein mediated resistance to drugs.<sup>8</sup> In order to discover some potential anticancer leading structure, Insuasty et al. synthesized a series of 3-aryl-2H-pyrazole derivatives in 2009.<sup>9</sup> And then, US National Cancer Institute screened some compounds of those derivatives inhibiting about 60 variety of human tumor cell lines.<sup>10</sup>

Oxygen-bearing heterocycles especially 1,3-benzodioxole and 1,4-benzodioxan have caught significant attention in the medicinal chemical research field.<sup>11</sup> The benzodioxole group is widely used in synthetic medicinal chemistry as a component of enzyme inhibitors; it is present in piperine, a known enzyme inhibitor. Besides,

more and more chemical compounds bearing 1,4-benzodioxan moiety as potential anticancer agents have been confirmed.<sup>12–14</sup> Relevant research indicated that 1,3,4-oxadiazole derivatives bearing 1,4-benzodioxan moiety show low toxicity to human liver cells and have a good inhibitory effect on cancer cells.<sup>15</sup>

Andrew et al. revealed the telomerase key active site with X-ray in 2008, which was three-dimensional structure of TERT protein catalysis subunit.<sup>3</sup> At present, our group designed and synthesized several kinds of telomerase inhibitors.<sup>16–18</sup> All of these compounds had the similar skeleton structure: 2H-pyrazole. So we deduced that 2H-pyrazole might be used as key group to show telomerase inhibitory activity.

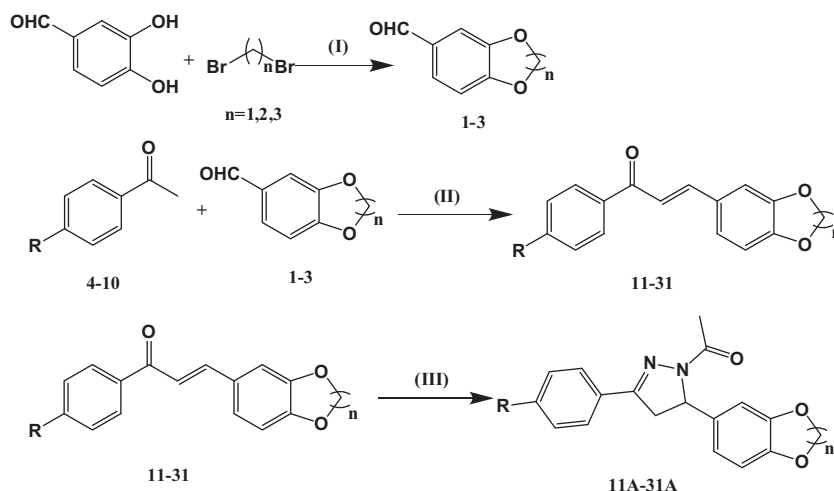
Above all, we continued our previous study and designed new 2H-pyrazoles bearing oxygen-bearing heterocycles targeting telomerase. In this Letter, we described the synthesis and the structure–activity relationships of series of aryl-2H-pyrazole derivatives bearing 1,5-benzodioxepine or 1,4-benzodioxan or 1,3-benzodioxole moiety as potential antitumor agents, which was based on molecular modeling. Biological evaluation was also carried out for screening potential telomerase inhibitors among the synthesized compounds. Docking simulations were performed using the X-ray crystallographic structure of the telomerase in complex with an inhibitor to explore the binding mode of the compound at the active site. Based on the activity data, QSAR model was also built to study the structure–activity relationship and guide the further study.

A series of novel aryl-2H-pyrazole derivatives were synthesized by the routes outlined in Scheme 1. Compounds **1–3** were synthesized from 3,4-dihydroxybenzaldehyde and dibromomethane or

\* Corresponding authors. Tel.: +86 25 8359 2572; fax: +86 25 8359 2672.

E-mail address: [zhuhl@nju.edu.cn](mailto:zhuhl@nju.edu.cn) (H.-L. Zhu).

† These two authors equally contribute to this work.



**Scheme 1.** Synthetic pathway of compounds **11A–31A**. Reagents and conditions: (I) acetone,  $K_2CO_3$ , reflux, 24 h; (II) EtOH, KOH (40% aq), rt 2 h; (III) hydrazine hydrate, acetic acid, reflux, 2 h.

dibromoethane or dibromopropane with acetone as solvent in the presence of potassium carbonate. The synthesized compounds were then reacted with substituted acetophenones (**4–10**) to prepare the corresponding chalcone derivatives **11–31**. After that solution of compounds **11–31** in acetic acid were reacted with hydrazine hydrate to synthesize corresponding *2H*-pyrazoles **11A–31A**. Compounds **17A–31A** reported synthesized for the first time. These compounds gave satisfactory elementary analyses.  $^1H$  NMR and ESI MS spectra were consistent with the assigned structures.

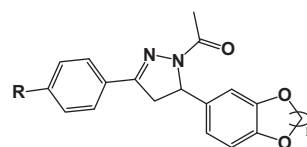
Compounds **11A–31A** were evaluated for telomerase inhibitory activities by a modified telomere repeat amplification protocol (TRAP) assay.<sup>20</sup> Modified TRAP assay was proved to be a useful technology to give some information about small molecules inhibiting telomere elongation qualitatively and quantitatively.<sup>20</sup> As summarized in **Table 1**, most of the synthesized *2H*-pyrazole derivatives displayed good telomerase inhibitory activities and among them compound **16A** displayed the best inhibitory activity with  $IC_{50}$  of 0.9  $\mu M$  for telomerase which could be comparable to the reference compound ethidium bromide.

According to the data presented in **Table 1**, it could be concluded that aryl-*2H*-pyrazole derivatives bearing 1,3-benzodioxole group (compounds **11A–17A**) displayed better telomerase inhibitory activities, whereas aryl-*2H*-pyrazole derivatives bearing 1,4-benzodioxan and 1,5-benzodioxepine group, in general, showed relatively worse activities. And the results suggested that the compounds with 1,3-benzodioxole group (**11A–17A**) and electron-donating groups in R position (**15A**, **16A**, **22A**, **23A**, **29A** and **30A**) showed better telomerase inhibitory activities than compounds with electron-withdrawing substituents. Some compounds in this series deserve further investigation.

Based on above results, compounds **11A–31A** were also chosen to finish the screening assay studies. These compounds were evaluated for their anticancer activities against gastric SGC-7901 (human gastric cancer) and B16-F10 (mouse melanoma) cell lines. From the results summarized in **Table 1**, it was obvious that compound **16A** exhibited best activity against B16-F10 cells with the  $IC_{50}$  value of 5.34  $\mu M$ , much better than the reference drug 5-fluorouracil with the  $IC_{50}$  value of 21.41  $\mu M$ . Most of the compounds bearing 1,3-benzodioxole (**11A–17A**) exhibited better activity against B16-F10 compared with reference drug. And also it was obvious that compounds bearing 1,3-benzodioxole (**11A–17A**) group showed better anticancer activity than those bearing 1,4-benzodioxan and 1,5-benzodioxepine groups. At the same time,

**Table 1**

Inhibitory effects of the title compounds against telomerase and cancer cell lines



Compounds	n	R	$IC_{50}(\mu M)$ B16-F10	$IC_{50}(\mu M)$ SGC-7901	$IC_{50}(\mu M)$ Telomerase
<b>11A</b>	1	H	13.96	25.67	3.4
<b>12A</b>	1	F	22.17	40.85	7.3
<b>13A</b>	1	Cl	20.83	35.33	6.7
<b>14A</b>	1	Br	18.93	30.09	6.2
<b>15A</b>	1	CH <sub>3</sub>	12.78	21.24	1.3
<b>16A</b>	1	OCH <sub>3</sub>	5.34	18.07	0.9
<b>17A</b>	1	NO <sub>2</sub>	24.74	41.93	8.7
<b>18A</b>	2	H	39.52	50.17	18.5
<b>19A</b>	2	F	53.11	68.39	25.7
<b>20A</b>	2	Cl	47.34	59.46	23.8
<b>21A</b>	2	Br	44.06	52.31	22.9
<b>22A</b>	2	CH <sub>3</sub>	37.93	49.22	13.4
<b>23A</b>	2	OCH <sub>3</sub>	31.67	45.83	10.6
<b>24A</b>	2	NO <sub>2</sub>	57.8	70.05	37.4
<b>25A</b>	3	H	No	No	68.3
<b>26A</b>	3	F	No	No	83.6
<b>27A</b>	3	Cl	No	No	82.6
<b>28A</b>	3	Br	96.95	No	76.4
<b>29A</b>	3	CH <sub>3</sub>	89.71	No	54.9
<b>30A</b>	3	OCH <sub>3</sub>	85.26	94.01	46.7
<b>31A</b>	3	NO <sub>2</sub>	No	No	93.2
5-Fluorouracil			21.41	46.35	
Ethidium bromide <sup>a</sup>					2.6

No, not observed in the tested concentration range 0–100  $\mu M$ .

<sup>a</sup> Ethidium bromide is reported as a control. The inhibition constant of ethidium toward telomerase has been reported previously.

in contrast, all the synthesized compounds exhibited worse activity against SGC-7901 cells. The results were similar with previous paper.<sup>21</sup>

Molecular docking is an application wherein molecular modeling techniques are used to predict how a protein (enzyme) interacts with small molecules (ligands).<sup>22</sup> In order to explore probable interaction model of inhibitors (ligands) and enzyme active site, molecular docking of the most potent enzyme inhibitor **16A** into active binding site of telomerase was performed to

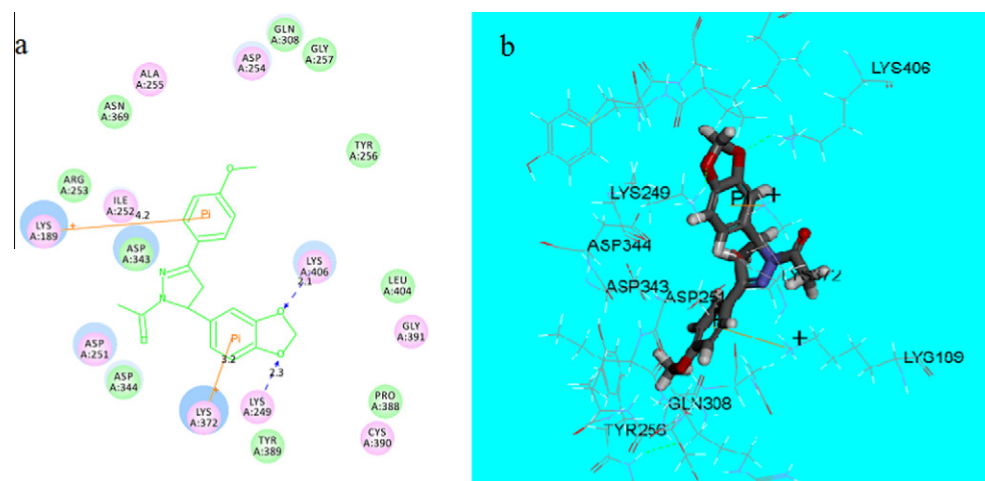


**Figure 1.** (a) Ligand interaction diagram of compound **16A** with TERT protein catalytic subunit (PDB ID: 3DU6) using Discovery Studio program with the essential amino acid residues at the binding site are tagged in circles. The purple circles show the amino acids which participate in hydrogen bonding, electrostatic or polar interactions and the green circles show the amino acids which participate in the van der Waals interactions. (b) The 3D model structure of compound **16A** binding model with telomerase complex.

**Table 2**

Experimental, predicted inhibitory activity of compounds **11A–31A** by 3D-QSAR models based upon active conformation achieved by molecular docking

Compound	Experimental pIC <sub>50</sub>	Predicted pIC <sub>50</sub>	Residual error
<b>11A</b>	5.469	5.200	0.269
<b>12A</b>	5.137	5.506	−0.369
<b>13A</b>	5.174	4.991	0.183
<b>14A</b>	5.208	5.523	−0.315
<b>15A</b>	5.886	5.702	0.184
<b>16A</b>	6.046	5.876	0.169
<b>17A</b>	5.060	4.702	0.359
<b>18A</b>	4.733	5.070	−0.337
<b>19A</b>	4.590	4.368	0.222
<b>20A</b>	4.623	5.027	−0.403
<b>21A</b>	4.640	4.621	0.020
<b>22A</b>	4.873	4.707	0.166
<b>23A</b>	4.975	4.704	0.270
<b>24A</b>	4.427	4.711	−0.283
<b>25A</b>	4.166	4.549	−0.383
<b>26A</b>	4.078	4.283	−0.205
<b>27A</b>	4.083	4.202	−0.119
<b>28A</b>	4.117	4.372	−0.255
<b>29A</b>	4.260	4.447	−0.187
<b>30A</b>	4.331	4.212	0.119
<b>31A</b>	4.031	4.075	−0.044

simulate a binding model derived from TERT protein catalytic subunit (3DU6.pdb).

All docking runs were applied CDOCKER protocol of Discovery Studio 3.1. The 2D and 3D binding model of compound **16A** and telomerase was depicted in Figure 1. In the binding model, compound **16A** was nicely bound to the TERT protein catalytic subunit with four interaction bonds with binding interaction energy of  $-35.76 \text{ kJ mol}^{-1}$ . Visual inspection of the pose of **16A** into the active site revealed that two optimal intermolecular hydrogen bonds were observed (LYS249: N–H...O: 2.3 Å, angle: 137.6°; LYS406: N–H...O: 2.1 Å, angle: 137.6°). Also the two benzene rings formed  $\pi$ -cation interactions with LYS189 and LYS372, respectively. These residues influenced the accessibility of the hydrophobic pocket that flanks the active binding site, and their size could be important in controlling telomerase selectivity. In the other end of the binding pocket, the oxygen atom of 2H-pyrazole acetyl interacted with the residue GLN308, which might make the 3D structure more stable.

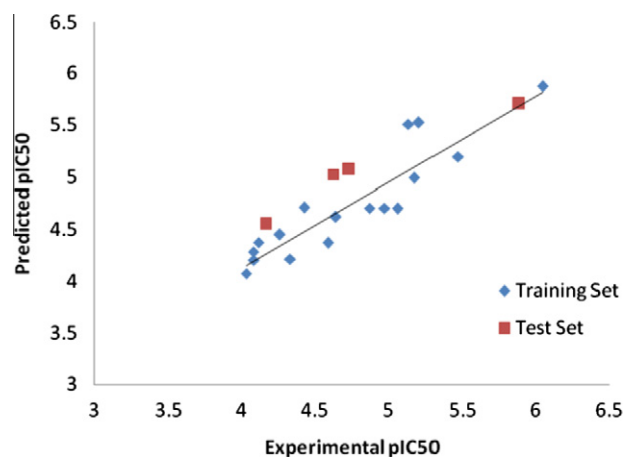


**Figure 2.** Plot of experimental versus predicted telomerase inhibitory activities of training set and test set.

Based on the preliminary biological results, a 3D-QSAR model of these 2H-pyrazole derivatives was initiated by using a novel 3D-QSAR protocol of Discovery Studio 3.1. The calculated pIC<sub>50</sub> values ranged from 4.08 to 6.04.

Twenty one compounds (Table 1) with IC<sub>50</sub>s ranging from 0.9 to 82.6  $\mu\text{M}$  for inhibiting telomerase were selected as the model dataset. The IC<sub>50</sub> values were converted into corresponding pIC<sub>50</sub> values by the formula in Eq. (1):

$$\text{pIC}_{50} = -\log_{10} \text{IC}_{50} \quad (1)$$

Because molecular alignment was considered as a crucial step for 3D-QSAR study,<sup>23</sup> we applied CDOCKER protocol to explore each molecule with lowest energy before alignment conformation. 4,5-Dihydro-1H-pyrazole was selected as substructure to build alignment conformation before building the QSAR model. The initial set of compounds has been randomly divided into training set and test set by the Molecules method in Discovery Studio.

The correlation coefficient  $r^2$  between observed and predicted activity of training set was found to be 0.829, while that of test set was found to be 0.966, which proved this QSAR model was acceptable. Predicted pIC<sub>50</sub> values and residual errors of 21 compounds by this QSAR model had been given in Table 2. The plot

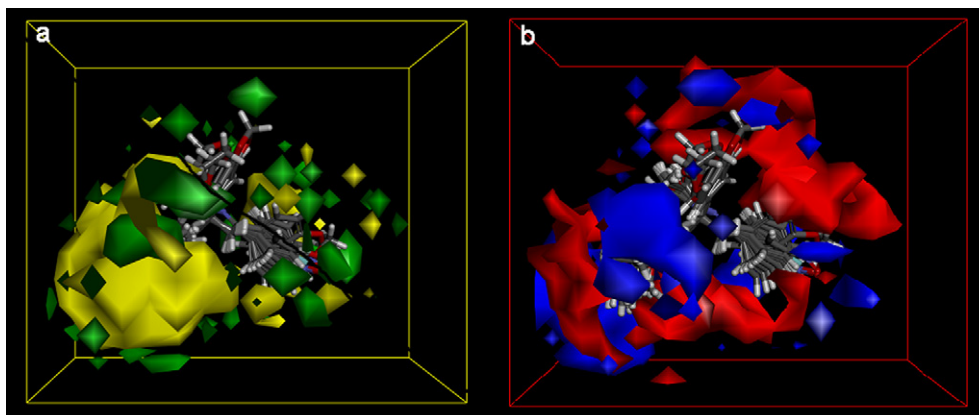


**Figure 3.** (a) 3D-QSAR model coefficients on van der Waals grids. Green represents positive coefficients; yellow represents negative coefficients. (b) 3D-QSAR model coefficients on electrostatic potential grids. Blue represents positive coefficients; red represents negative coefficients.

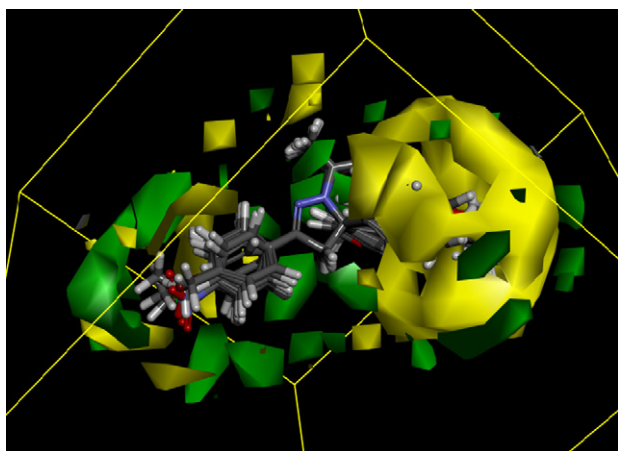


**Figure 4.** 3D-QSAR model coefficients on van der Waals grids from another perspective.

of the observed  $pIC_{50}$  versus the predicted data was shown in Figure 2. Besides, we have built a random model by adding two reported compounds in previous paper (4a and 4b in reference<sup>18</sup>). The results showed that  $r^2$  for training set was 0.984 and that of test set was 0.567 while that of test set was 0.996 in statistical model. This model could lead to increase residual errors. We can assure that the statistical model is much more reliable than random model.

Also the molecules aligned with the iso-surfaces of the 3D-QSAR model coefficients on van der Waals grids (Fig. 3a) and electrostatic potential grids (Fig. 3b) are listed. Electrostatic map indicates red contours around regions where high electron density (negative charge) is expected to increase activity, and blue contours represent areas where low electron density (partial positive charge) is expected to increase activity. Similarly, steric map indicates areas where steric bulk is predicted to increase (green) or decrease (yellow) activity.

According to the maps, it suggested the compound with high positive charged and small oxygen-bearing heterocycle group would show higher activity, validating that 1,3-benzodioxole group being a better choice than 1,4-benzodioxan and 1,5-benzodioxepine. Whereas, a high negative charged R group would help obtain good activity, validating the methoxy substituent could be more effective. As shown in Figure 4, it was clear that R groups were surrounded by several green and yellow grids, which suggested that molecular size did not influence the activity obviously.

As a result, data summarized above demonstrated that compounds **16A**, the most potent telomerase inhibitor ( $IC_{50} = 0.9 \mu M$ ), containing suitable substituents had an outstanding activity.

In all, a series of novel aryl-2*H*-pyrazole derivatives bearing oxygen-bearing heterocycle group were prepared as potential telomerase inhibitors. The bioactivity assay results showed that compound **16A** showed most potent inhibition activity for telomerase and good activity against human melanoma cell B16-F10 better than reference drug. Docking simulation was performed to position compound **16A** into 3DU6 active site, the result showed compound **16A** could bind well with the telomerase active site and act as telomerase inhibitor. QSAR model was also built by the activity data and binding conformations to provide a reliable tool for rational design of novel telomerase inhibitors. The above results provided theoretical basis for further structural optimization of 2*H*-pyrazole derivatives as telomerase inhibitors.

#### Acknowledgment

This work was supported by the National Natural Science Foundation of China (Grant Nos. 20371050, 21273283 and J1103512).

#### Supplementary data

Supplementary data associated with this article can be found, in the online version, at <http://dx.doi.org/10.1016/j.bmcl.2012.12.010>.

#### References and notes

1. Wright, W. E.; Shay, J. W. *Curr. Opin. Genet. Dev.* **2001**, *11*, 98.
2. Bodnar, A. G.; Ouellette, M.; Frolkis, M.; Holt, S. E.; Chiu, C. P.; Morin, G. B.; Harley, C. B.; Shay, J. W.; Lichtsteiner, S.; Wright, W. E. *Science* **1998**, *279*, 349.
3. Andrew, J. G.; Anthony, P. S.; Emmanuel, S. *Nature* **2008**, *455*, 633.
4. Liu, X. H.; Ruan, B. F.; Li, J.; Song, B. A.; Zhu, H. L.; Bhadury, P. S. *Mini-Rev. Med. Chem.* **2011**, *11*, 771.
5. Girisha, K. S.; Kalluraya, B.; Vijaya, N.; Padmashree *Eur. J. Med. Chem.* **2010**, *45*, 4640.
6. Hayat, F.; Salahuddin, A.; Umar, S.; Azam, A. *Eur. J. Med. Chem.* **2010**, *45*, 4669.
7. Boyer, F. E.; Vara Prasad, J. V. N.; Choy, A. L.; Chupak, L.; Dermeyer, M. R. *Bioorg. Med. Chem. Lett.* **2007**, *17*, 4694.
8. Havrylyuk, D.; Zimenkovsky, B.; Vasylenko, O.; Zaprutko, L.; Gzella, A.; Lesyk, R. *Eur. J. Med. Chem.* **2009**, *44*, 1396.
9. Shaharyar, M.; Abdullah, M. M.; Bakht, M. A.; Majeed, J. *Eur. J. Med. Chem.* **2010**, *45*, 114.
10. Insuasty, B.; Tigreros, A.; Orozco, F.; Quiroga, J.; Abonía, R.; Nogueras, M.; Sanchez, A.; Cobo, J. *Bioorg. Med. Chem. Lett.* **2010**, *18*, 4965.
11. Lv, P. C.; Wang, K. R.; Mao, W. J.; Xiong, J.; Li, H. Q.; Yang, Y.; Shi, L. *ChemMedChem* **2009**, *4*, 1.
12. Vazquez, M. T.; Rosell, G.; Pujol, M. D. *Farmacologia* **1996**, *51*, 215.

13. Harrak, Y.; Rosell, G.; Daidone, G.; Plescia, S.; Schillaci, D.; Pujol, M. D. *Bioorg. Med. Chem. Lett.* **2007**, *15*, 4876.
14. Xu, M. Z.; Lee, W. S.; Han, J. M.; Oh, H. W.; Park, D. S.; Tian, G. R.; Jeong, T. S.; Park, H. Y. *Bioorg. Med. Chem. Lett.* **2006**, *14*, 7826.
15. Zhang, X. M.; Qiu, M.; Sun, J.; Zhang, Y. B.; Yang, Y. S.; Wang, X. L.; Tang, J. F.; Zhu, H. L. *Bioorg. Med. Chem. Lett.* **2011**, *19*, 6518.
16. Liu, X. H.; Liu, H. F.; Shen, X.; Song, B. A.; Zhu, H. L. *Bioorg. Med. Chem. Lett.* **2010**, *20*, 4163.
17. Liu, X. H.; Liu, X. F.; Chen, J.; Zhu, H. L. *Bioorg. Med. Chem. Lett.* **2010**, *20*, 5705.
18. Liu, X. H.; Ruan, B. F.; Liu, J. X.; Song, B. A.; Zhu, H. L. *Bioorg. Med. Chem. Lett.* **2011**, *21*, 2916.
19. Kim, N. W.; Piatyszek, M. A.; Prowse, K. R.; Harley, C. B.; West, M. D.; Ho, P. L.; Coviello, G. M.; Wright, W. E.; Weinrich, S. L.; Shay, J. W. *Science* **1994**, *266*, 2011.
20. Han, H.; Hurly, L. H.; Salazar, M. *Nucleic AcidS Res.* **1999**, *27*, 537.
21. Insuasty, B.; Chamizo, L.; Munoz, J.; Tigreros, A.; Quiroga, J.; Abonia, R.; Noguerras, M.; Cobo, J. *Arch. Pharm. Chem. Life Sci.* **2012**, *345*, 275.
22. Kirkpatrick, P. *Nat. Rev. Drug Disc.* **2004**, *3*, 299.
23. Kothandana, G.; Gadhe, C. G.; Madhavan, T.; Choi, C. H.; Cho, S. J. *Eur. J. Med. Chem.* **2011**, *46*, 4078.